Probing the Limits of PON Monitoring Using Periodic Coding Technology

Mohammad M. Rad, *Member, IEEE*, Julien Penon, *Member, IEEE*, Habib A. Fathallah, *Member, IEEE*, Sophie LaRochelle, *Member, IEEE, Member*, and Leslie A. Rusch, *Fellow, IEEE*

***Abstract*—We probe the limits, both experimentally and analytically, of passive optical network (PON) monitoring using periodic coding technology. The experimental demonstration focuses on a 16 customer PON with a 20 km feeder fiber followed by either a single cluster or a tiered hierarchy. A directly modulated laser modulated at 1 GHz was used to generate the monitoring probe signals. The measured data from the experimental setup was fed to a reduced complexity maximum likelihood sequence estimation (RC-MLSE) algorithm to detect and localize the customers. Three different PON deployments were tested. We demonstrate improved monitoring robustness when using a variable threshold for networks with a tiered geographic distribution. While only a 16 customer PON was tested, our experimental setup had 18 dB margin in the total loss budget corresponding to splitting losses for 64 customers. We investigate analytically the total permissible loss budget of the monitoring system operating in the 1650 nm waveband as a function of receiver specifications. We examine the effect of resolution in the analog-to-digital conversion on the correlation peaks that form sufficient statistics for the RC-MLSE algorithm. Resolution affects both the RC-MLSE algorithm and the use of signal averaging to improve signal-to-noise ratio. We find that the monitoring system is able to monitor current PON standards with inexpensive, commercially available electronics.**

***Index Terms*—Analog-to-digital converter (ADC), loss budget, maximum likelihood sequence estimation (MLSE), network monitoring, optical coding (OC), periodic code, passive optical network (PON).**

I. Introduction

CODING has been proposed for monitoring of passive optical networks (PONs) [1]–[4]. Faulty fiber lines are identified by the absence of their coded return signals. Most importantly, such systems are self-configuring: they blindly identify the position of all network subscribers based solely on knowledge of the codes, and without knowledge or control of the installed fiber lengths. The self-configuration (and subsequent fault identification) must be achieved in a reasonable time period (seconds to minutes) to be of practical interest. Our previous studies have quantified via simulation how the geographical topology of the network impacts the processing time for the monitoring system [2], [5]. We present experimental validations of those predictions and demonstrate robust self-configuration in the case of tiered PONs.

Our previous analysis identified two factors impacting performance: 1) the complexity of the self-configuration; and 2) technological challenges. These two factors were sometimes interdependent. In particular, two scenarios could lead to excessive computation for self-configuration: extremely dense PONs and extremely distributed PONs. On the technology side, when PONs were excessively far flung, the monitoring signal exhibited large extremes in pulse heights from different subscribers. The more distant subscribers required more sensitivity at the receiver. Increased sensitivity makes self-configuration conceivable, but may be impossible to achieve due to high complexity. In this paper, we examine to what extent these limitations are likely to impact PON monitoring performance; this examination includes: 1) experimentation; 2) simulation; and 3) power budget analysis.

The experimental validation of the monitoring of extremely dense PONs was reported in [2] and [5], but suffered from severe technology challenges. The monitoring probe signal was generated by external modulation of a spectrally sliced broadband source leading to severe relative-intensity noise (RIN) as well as dispersion. External modulation also imposes significant insertion loss and poor extinction ratios. In this paper, we adopt direct modulation of a laser for better extinction ratio and less loss, improving the total system loss budget. With a coherent source both dispersion and RIN are negligible for PON monitoring. With these improvements, we examine a larger, more realistic yet geographically dense PON (16 customers versus four customers in the [2], [5] experiment). We also examine experimentally extremely disperse PONs for the first time.

Whether using incoherent or coherent sources, detection noises such as relative intensity, beat, and shot noises can be reduced by the averaging technique commonly used in optical time-domain reflectometer (OTDR) systems [2], [5]. The received signal can be considered virtually free of these noise sources, as we shall demonstrate. Interference from simultaneous returns from multiple customers is the primary source of noise. This interference is the source of extreme complexity in deciphering some PON topographies. From a technological point of view, the extremely low noise (other than interference)

Manuscript received June 28, 2010; revised September 09, 2010; accepted January 10, 2011. Date of publication March 10, 2011; date of current version April 20, 2011.

M. M. Rad is with the Department of Electrical and Computer Engineering, University of Waterloo, Waterloo, ON N2L 3G1, Canada (e-mail: mmmansou@uwaterloo.ca).

J. Penon is with Averna, Montreal, QC G1K 7P4, Canada (e-mail: julien.penon@averna.com).

H. A. Fathallah is with the Department of Electrical Engineering, College of Engineering, King Saud University, Riyadh 11451, Saudi Arabia, and also with the Department of Electrical and Computer Engineering, Laval University, Quebec, QC G1V 0A6, Canada (e-mail: hfathallah@ksu.edu.sa).

S. LaRochelle and L. A. Rusch are with the Department of Electrical and Computer Engineering and the Center for Optics, Photonics, and Lasers (COPL), Université Laval, Quebec, QC G1V 0A6, Canada (e-mail: sophie.larochelle@gel.ulaval.ca; larusch@ulaval.ca).

Color versions of one or more of the figures in this paper are available online at http://ieeexplore.ieee.org.

Digital Object Identifier 10.1109/JLT.2011.2125946

does not guarantee the receiver is capable of discerning all returns. The receiver sensitivity is still limited by the postdetection circuits, i.e., the transimpedance amplifier (TIA) gain and the resolution of analog-to-digital converter (ADC). The ADC resolution is considered to be the final system bottleneck. We will illustrate how the ADC resolution and the TIA gain play important roles in the maximum allowable loss budget of the network.

In Section II, we briefly introduce fiber link monitoring of a PON using periodic coding technology. In Section III, we review quantitative measures of the acceptable complexity in network self-configuration, and how various PON topographies could lead to excessive complexity. We focus on three topographical regions of interest for our experimental efforts. In Section IV, the experimental setup is described and results are presented. In Section V, we study theoretically the maximum allowable loss budget of our PON monitoring system based on current and future technologies.

II. PON Monitoring With Periodic Coding

Coding can be used to distinguish individual returns that would normally be superimposed and indistinguishable [1]. For PONs, this allows a single ping to the network to provide information on all tributary paths. Cost and complexity pose formidable obstacles, especially for the hardware (encoders) that must be deployed to every subscriber. For this reason, periodic codes were developed as they are both simple to fabricate and provide easily distinguishable returns. Their properties are described more fully in [4].

As mentioned in Section I, the performance of coding for monitoring is influenced by two critical factors: 1) the density of the network (the extent to which subscriber returns are closely packed); and 2) network geographical area (determining the greatest attenuation of returns). Implicit in these two factors is the number of subscribers; for example, a large number of subscribers in a small coverage area will clearly lead to dense returns. Let N be the number of customers served, and Δl be the maximum relative distance (separation) between the customers in the network in meters. We can say that the size of the network (taking into account both customers served N and geographical coverage parameterized by Δl) determines to what extent the self-configuration is challenging.

We proposed a reduced complexity maximum likelihood sequence estimation (RC-MLSE) to configure the network, i.e., to ascertain the positions of all subscribers by identifying each unique code return in the cacophony of superimposed codes returned by the network [2], [5]. Given sufficient processing time, any network could be configured with sufficient averaging to significantly improve signal-to-noise ratio (SNR); RIN, beat noise, thermal noise, and shot noise are essentially eliminated leaving only interference, dark current, and quantization noise. For a sufficiently sensitive receiver, detection would be error free given sufficient processing time. Some network topologies, however, will present interference that causes the processing time to exceed a practical bound. In order to assess the robustness of our algorithm, in [5], we completed Monte Carlo simulations to quantify processing time required for a statistical distribution of network topologies.

In [5], we examined via simulation a wide range of network sizes (geographic and clientele supported), identifying combinations of coverage area and customer number that led to timing out in the reduced complexity receiver. We also proposed the use of a variable threshold for tiered deployments to reduce the time-out occurrence, although this was not investigated in that work. A detailed study of the efficiency of the proposed RC-MLSE algorithm can be found in [5]. In this paper, we focus on network sizes that can be studied experimentally, and yet also clearly exhibit interference limited and threshold limited regions. To wit, we selected 8 and 16 customer networks.

We first simulate the 8 and 16 customer network time-out probability. We fixed the acceptable processing delay to 2 min when using a MATLAB implementation of our algorithm on a 2.3 GHz dual core Pentium. The code was not optimized, and runtime could undoubtedly be improved. However, our goal was simply to quantify a reasonable limit on complexity that could be handled by the algorithm. Our pulsewidth was one nanosecond and we assumed Nyquist sampling at $R_s = 2$ Gs/s.

We swept through geographical coverage parameterized by Δl. We assumed that the network topology followed a uniform radial distribution over an area of $\pi \Delta l^2$. For each of the N customers, we randomly generated a position within the circular coverage area and assigned each a periodic code. The response of this network to a $T_s = 1$ ns pulse was generated and fed to our reduced complexity MLSE to identify the network configuration. Those configurations where processing delay would have exceeded 2 min were noted. Statistics were generated giving the time-out probability P_{TO} (probability that the RC-MLSE could not handle the topology in 2 min), or equivalently, the percentage of networks that caused a time-out to occur. The results are presented in Fig. 1.

In Fig. 1, we see that for $N = 8$ customer PON, P_{TO} is high only for very large Δl, (≥ 5 km). For $N = 16, P_{\mathrm{TO}}$ is high for both very small and very large Δl; for moderate values of $\Delta l, P_{\mathrm{TO}}$ is minimal. We have identified two regions of interest: to the left an interference-dominated region exists, while to the right a region we call threshold limited. As expected, very small coverage areas leads to code returns that are highly superimposed (high interference) and causing the MLSE algorithm to consider an excessively large number of possible network configurations. Note that the interference limited region is actually so dense that it would exclude single family home deployments [5].

The second (upper) x axis gives the maximum relative loss, i.e., the difference in received powers of weakest and strongest returns assuming fiber attenuation of 0.3 dB/km in each direction when using the *U*-band [6]. For a large coverage area, the upper axis shows how the loss increases, forcing the threshold to be set lower to detect the weakest code returns. The lower threshold leads to false "positive hits" in the RC-MLSE algorithm; nominally empty portions of the return are considered possible codes, leading to time-outs. While periodic codes have a limited number of dominant return pulses, secondary returns are causing the false positives. In practical PON deployments, customers are typically distributed in different geographical tiers [7]. Each tier supports a local grouping of subscribers. For tiered deployments, we can greatly reduce P_{TO} by exploiting

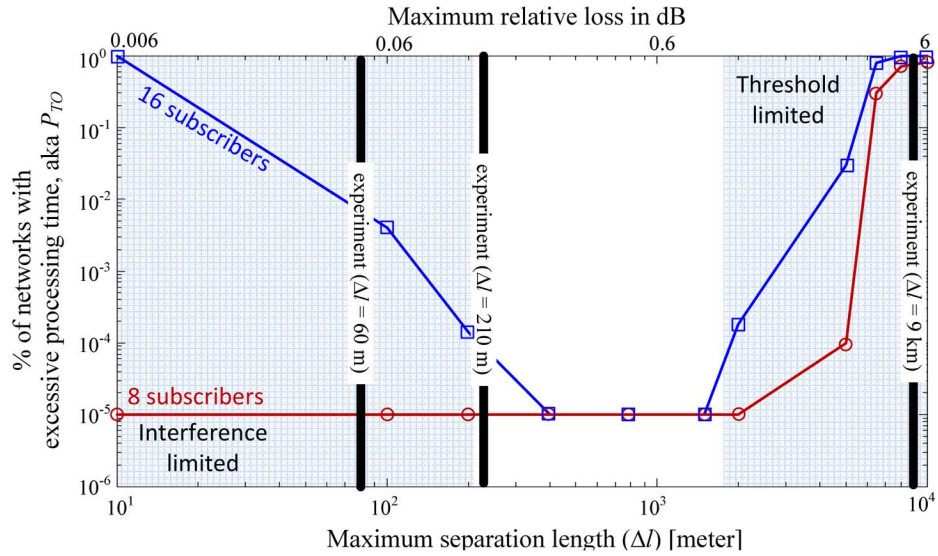

Fig. 1. Monte Carlo simulation for time-out probability versus maximum separation length Δl for 8 and 16 customer PON using periodic codes.

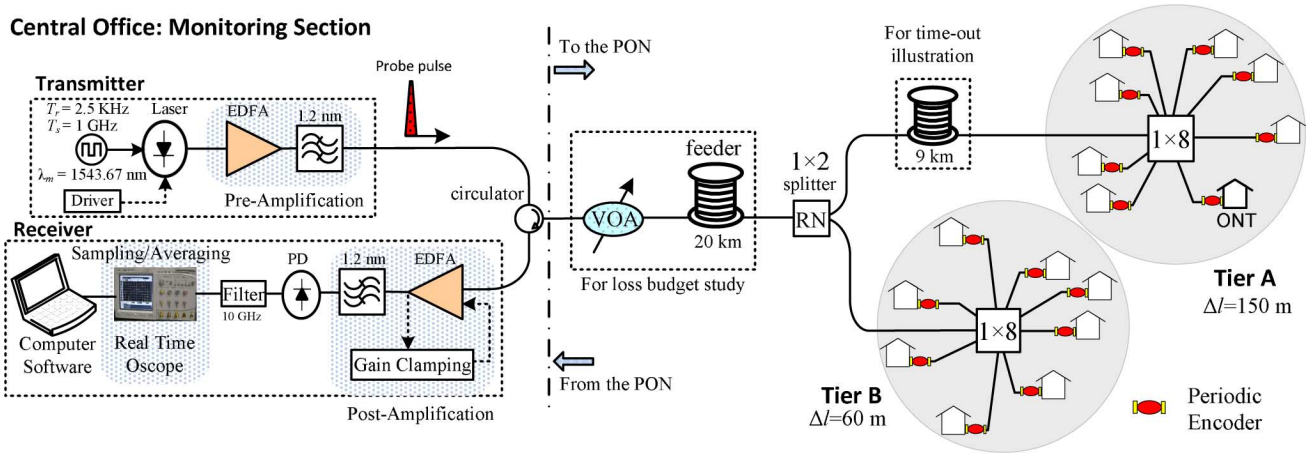

Fig. 2. Experimental setup for PON monitoring using periodic coding technology.

information on the distance between tiers. The threshold can be adjusted for these clustered returns, avoiding false positives [5].

III. Experimental Demonstration

We selected three network configurations for experimental validation; as marked in Fig. 2, one in each of the three regions of operation. In the interference free region (eight-user tier B) and the middle region (eight-user tier A and eight-user tier B), the network configuration chosen did not result in a time-out. In the third case, the configuration (tier B at the same distance, but tier A located at a greater distance) led to a threshold with an excessive time-out.

For our experimental demonstration, we fabricated $N = 16$ periodic encoders. Each encoder consists of two gratings: the first is partially reflective (38%) while the second acts like a mirror (100% reflectivity). Each grating has a rejection bandwidth of $d = 12$ nm with center wavelength of 1550 nm [2]. For effective code weight $w = 4$ and maximum cross-correlation $\lambda_c = 1$, we produced codes with periodicity $p_i \in \{6, 7, 11, 13, 16, 17, 19, 23, 25, 27, 29, 21, 27, 41, 42, 43\}$ [4]. We excluded the code with periodicity of one due to difficulty in fabrication. The periodicity p_i determines the required patchcord length to make periodic encoders. Given a pulsewidth $T_s = 1$ ns, we constructed the appropriate length patch cord between each grating pair to make the periodic encoders [2].

A. Experimental Setup

The experimental setup is shown in Fig. 2. The central office generates pulses and processes the return signal. The network is a $l_f = 20$ km feeder followed by passive splitting and fiber drops; each of the (up to) sixteen subscribers has a distinct periodic encoder. A directly modulated laser with center wavelength of $\lambda_m = 1544.67$ nm and extinction ratio $\epsilon_r = 18.2$ dB generates the monitoring pulses. The laser is driven at a repetition interval of $T_r = 400$ μs ($R_r = 2.5$ kHz). The modulated signal is preamplified by an erbium-doped fiber amplifier (EDFA). Optical filter ($B_o = 1.2$ nm) is used after the EDFA to suppress the amplified spontaneous emission (ASE) noise. The received data are also postamplified at the CO. The postamplification is more critical as the received pulses are very weak. More importantly,

because the subscribers are located at different distances, the received pulse intensities vary. Recall that the encoded sequence coming from a specific coding mirror also has pulses with different amplitudes [4]. Therefore, a clamping circuit is necessary to keep the EDFA at an optimal operating point so as all the received pulses observe the same amplification gain; hence minimizing the distortion and nonlinear effects. The virtual lasing circuit (at the clamping segment) operating at 1559.85 nm uses the ASE of the post-EDFA to keep the total input power constant (see Fig. 2).

Due to equipment availability, we are operating at the 1550 nm window instead of 1650 nm window [2]. The monitoring pulse is sent to the network using a circulator (with 3 dB total insertion loss). The 1×2 coupler serves as the first remote node (RN). Due to the round trip of the monitoring pulse through the network, the total insertion losses of passive components are doubled, i.e., 2×4 dB for 1×2 splitter, 2×10 dB for 1×8 splitter and $2 \times 20 \times 0.2$ dB for 20 km feeder fiber. A real-time oscilloscope sampling at 10 Gs/s was used to capture the measured trace. The oscilloscope provides both sampling and averaging (up to 4096).

B. Simulation Results

We demonstrated three different geographical deployments: 1) $N = 8$ customer within $\Delta l = 60$ m; 2) $N = 16$ customers within $\Delta l = 210$ m; and 3) $N = 16$ customers within $\Delta l = 9$ km; the physical distances were selected randomly and then fixed for the experiment. The measured data from our experimental setup in Fig. 2 were fed into our algorithm to determine the network configuration [2]. For $N = 8$ with $\Delta l = 60$ and $N = 16$ with $\Delta l = 210$ m, the customers are easily identified (error free and within a few centimeters resolution [2]); hence no time-out. Note that P_{TO} is very small for these regions of Δl, i.e., less than one per 10^4 realizations per Fig. 1.

For $N = 16$ with $\Delta l = 9$ km (this exaggerated distance was used to assure we encountered a time-out), we realized a PON deployment consisting of two tiers, namely A and B (separated by $l_{\mathrm{AB}} = 9$ km), each of which supports eight subscribers per Fig. 2. The measured data fed into the RC-MLSE algorithm caused the algorithm to experience a time-out, i.e., the processing delay is larger than 2 min. The threshold was lowered to avoid missing a weak return, causing an excessive number of false positives to be searched. When using *a priori* information about the deployment, the time-out was eliminated.

The return signal was split into two returns to be processed separately: a return from before the l_{AB} fiber separation, and a return from the more distant tier. The low threshold was not used on the strong return from the closer tier, but only on the more distant return. Once again, we achieved error-free performance with resolution of each customer fiber length to within a few centimeters.

Most reasonably sized networks will not experience time-out (statistics shown in Fig. 1). They will fall in the white zone of Fig. 1. The interference limited region is so dense as to exclude single family home deployments. In multiple home dwellings, tiering of clients could be used to move from the interference limited zone to the white zone. The small percentage of deployments that are threshold limited (zone to right in Fig. 1) must employ side information. In this experiment, we validated the use of side information in the form of separation of clients in a tiered deployment. Other types of side information can be employed. For instance, for a strictly cluster deployment a sliding threshold could be used where the threshold diminished linearly, with slope determined by the level of attenuation with distance of the deployed fiber.

C. Loss Budget

We studied the loss budget of our monitoring system for future capacity expansion and/or longer reach PONs [6], [8]. For this purpose, a variable optical attenuator (VOA) is added to the setup in Fig. 2 followed by a $l_f = 20$ km fiber feeder. In each step, the insertion loss of the VOA is increased and the postamplification circuit is adjusted to properly detect the monitoring pulses. Our setup provides 9 dB margin (total of 18 dB for the round-trip path) for the loss budget; hence, the capacity can be scaled up by factor four via 1×4 splitter. Our experimental setup could therefore support a 64 customer PON with 20 km feeder fiber corresponding to current GPON standards [6]. Note that the sensitivity of the receiver is limited by the minimum detectable dc power at the receiver. The sensitivity of our monitoring system can be improved by using detectors with higher gains [15].

IV. Fundamental Limits of Loss Budget

Due to the round-trip path of the monitoring pulses, the insertion loss of passive elements is doubled, imposing strict limitations on the total loss budget of our monitoring system. We assume that a higher number of customers leads directly to higher splitting ratios at the RN and a more critical power/loss budget. Our experiments were carried out in the 1550 nm band for experimental convenience where amplification is straightforward. When deployed, a monitoring system will use the *U*-band where no amplifier exists, hence no pre- and postamplification such as that in Fig. 2 is possible. Therefore, the loss budget of our monitoring approach is a serious concern. In this section, we explain how averaging can help to improve the loss budget for the monitoring system. We also address the requirements for postdetection circuits to efficiently perform averaging. We then formulate the loss budget limit as a function of the corresponding circuit specifications.

A. Importance of Averaging

Increasing the transmitted power of the monitoring signal to mitigate the loss budget increases nonlinear effects, and cannot be employed without restraint. Indeed, to avoid nonlinear impairments, the launched power should be kept smaller than approximately 10 dBm for single mode fiber [8]. Our strategy for improved loss budgets relies on signal averaging. By averaging over many traces, i.e., repeating the measurement many times, we reduce noise and increase our SNR [8]. Hence, similar to standard OTDR techniques, the dynamic range and sensitivity of the monitoring receiver increases significantly. Assuming independent measurements, the noise power σ_n^2 is reduced proportionally by the number of measurements averaged M, i.e., $\sigma_n^2/(M)$. For a very large number of independent traces, $M \gg 1, \sigma_n^2/(M)$ tends to zero.

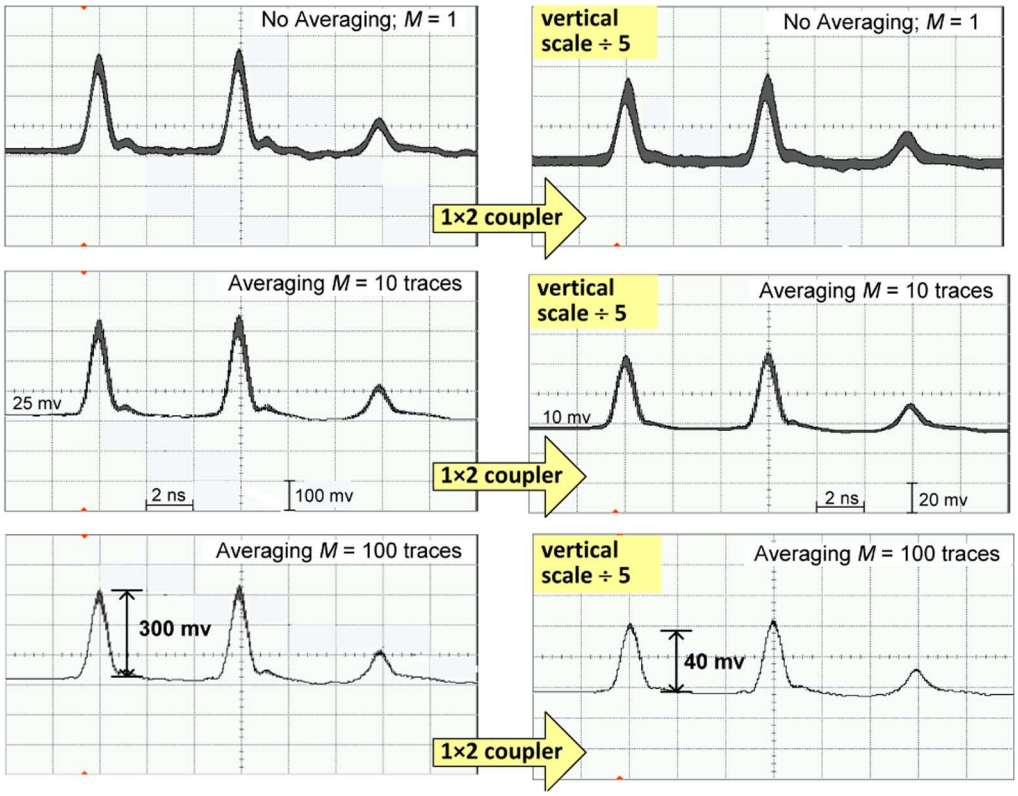

Fig. 3. Importance of averaging to improve the quality of the received monitoring sequences; traces averaged are $M = 1,\ 0,\ 00$.

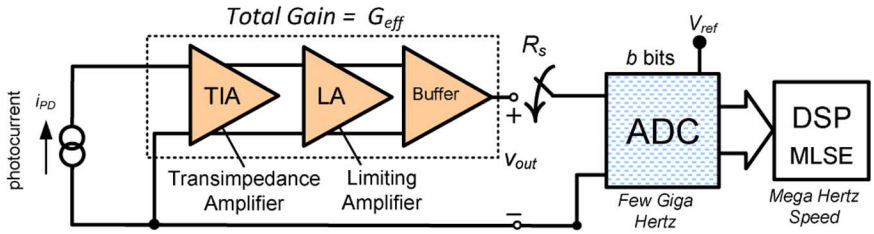

Fig. 4. Typical optical receiver using TIA and ADC.

A moderate delay for averaging and processing (milliseconds to seconds) is acceptable for our application; the temporal overhead for averaging is not burdensome. For example, consider a PON with 20 km reach length and a delay tolerance of 100 ms. In this case, the repetition rate R_r should be smaller than the total round-trip time for monitoring pulses, $R_r \leq 5$ kHz. A total of 500 traces can be averaged in 100 ms, for a 27 dB SNR enhancement [8].

Fig. 3 shows the response to a 1 ns probe pulse to the periodic encoder with $p_1 = 6$ ns, as measured using the setup in Fig. 2 and averaging over different number of traces M (different rows). The right column shows the same measurements but with an additional 6 dB loss due to a 1×2 coupler in the round-trip path; this illustrates the effect of degradation in the loss budget. In both columns, we see that increasing the number of traces being averaged improves the quality of the trace. In particular, for higher losses (right column), the noise is completely removed from the trace by $M = 100$ averaging (a 20 dB SNR improvement). Hence, error-free performance is achievable by the RC-MLSE algorithm [2], [5].

Signal averaging allows detection of very weak signals, however, receiver sensitivity is limited by postdetection circuits. Digital signal processing in the reduced complexity MLSE algorithm requires the monitoring signal be quantized. The quantization ultimately limits the amount of loss that can be sustained at the receiver without impairing the algorithm. As seen in Fig. 3, the small third pulse is virtually noise free, however, quantization must be sufficient to detect this small signal.

A typical postdetection circuit is illustrated in Fig. 4. The transimpedance or shunt amplifier (TIA) generates a voltage signal from the current produced by the photodiode $i_{\rm PD}$ [9], [10]. The TIA acts as a current to voltage converter with some amplification, and is widely used as a preamplifier in optical receivers. Typically, the TIA should have low noise and high dynamic range. Our application is insensitive to TIA noise due to averaging, thus relaxing this requirement. The TIA output is further amplified by a limiting amplifier that assures the output signal reaches the proper voltage range for the ADC. The total effective gain $G_{\rm eff}$ of all stages shown in Fig. 4 varies from 30 to 70 dB depending on the application [11], [12]. The

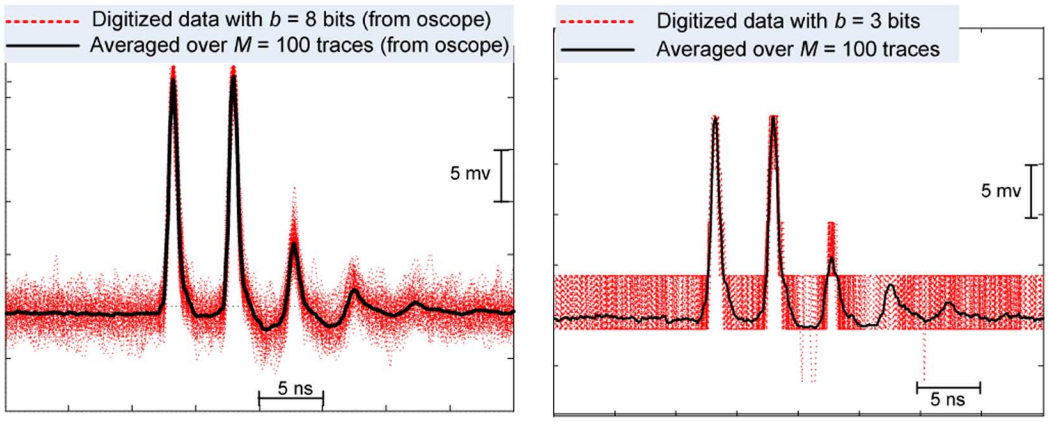

Fig. 5. Trace for periodic code with $p_1 = 6$ ns in a 16 customer network with a 20 km of fiber feeder; different levels of quantification (left 8 bits, right 3 bits) are shown for traces before and after $M = 100$ averaging.

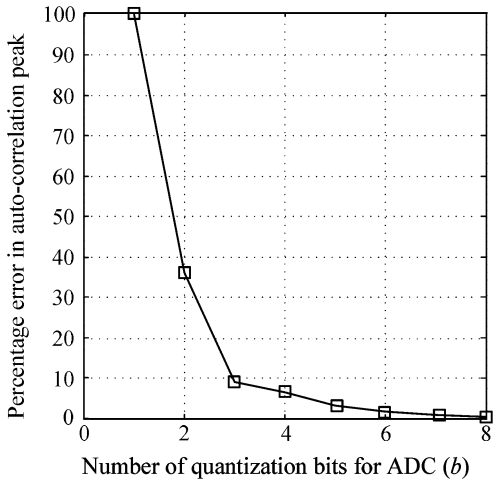

Fig. 6. Percentage of the error in estimating the autocorrelation peak as a function the number of quantization bits.

number of bits of resolution in the ADC is a design parameter. In Section IV-B, we illustrate how the ADC resolution affects the averaging process. The importance of G_{eff} is addressed in Section IV-C.

B. Quantification Effects

To illustrate the impact of ADC resolution, in Fig. 5, we examine the effect of averaging over 100 traces for two different ADCs. The trace to the left in Fig. 5 is captured by an Agilent Infinium 54845A real-time oscilloscope with $b = 8$ bits of resolution. The captured data are then requantified for a limited number of bits ($b = 3$); on the right in Fig. 5, we see the roughly quantized data and the averaged signal.

In order to ascertain the sensitivity of our detection algorithm to quantification levels, we focus our attention on code correlation. Correlation of the incoming monitoring signal with each code in turn generates the test statistics used for detection [2], [5]. Starting from the 8 bit digital signal captured from the real-time oscilloscope (shown in the left in Fig. 5), we reduced the number of bits progressively. For each resolution, the measured data from oscilloscope were quantized for $M = 100$ traces. We then averaged the quantized traces and calculated the degradation in the peak level of the correlation. The percentage of the error in estimating the autocorrelation peak as a function the number of quantization bits is shown in Fig. 6. For $b < 3$, we can see that averaging is ineffective and error is very high. For $b = 7$, the error is less than one percent. A good compromise to reduce cost of the receiver and digital signal processing is $b = 3$ where error is below ten percent. In Fig. 5, we can see that both levels of quantization yield good SNR improvement due to averaging[1].

C. Sensitivity of the Monitoring Receiver

The sensitivity of the receiver depends on both the TIA gain G_{eff} and the number of ADC quantization bits b. We have two requirements for error-free performance: 1) the averaging should reduce noise effectively; and 2) the first four pulses from each periodic encoder should be distinguishable following ADC. As explained in Section IV-B, a minimum of $b = 3$ bits assures SNR improvement with averaging. For the second requirement, recall that peak heights differing by less than V_{LSB} are indistinguishable, where V_{LSB} corresponds to the voltage of the least significant bit (LSB) [13]. For an ADC with b quantization bits, we have $V_{\text{LSB}} = V_{\text{ref}}/2^b$ where V_{ref} is the reference voltage [16].

For the periodic encoded sequence, more than 95% of the energy is concentrated in the first four pulses; thus it is sufficient to discern these four pulses [4]. The code characteristics are such that discerning the fourth pulse assures all four pulses are distinguishable. Thus, we require that the difference in the peak power between the fourth pulse and the remaining (weaker) pulses be greater than V_{LSB}. These pulses are dominated by the fifth pulse; the amplitudes of the fourth and fifth pulses (with respect to the unit height first two pulses) are 0.146 and 0.056 [4].

Now consider a monitoring system with a transmitted peak power of P_s, total insertion loss of α_T, and a U-band detector with responsivity R. Based on these discussions, we should have

$$\alpha_T R G_{\text{eff}} P_s (0.146 - 0.056) \geq V_{\text{LSB}} \tag{1}$$

[1]Simulations show that for additive Gaussian noise, $b = 3$ is sufficient to estimate the mean with less than one percent error.

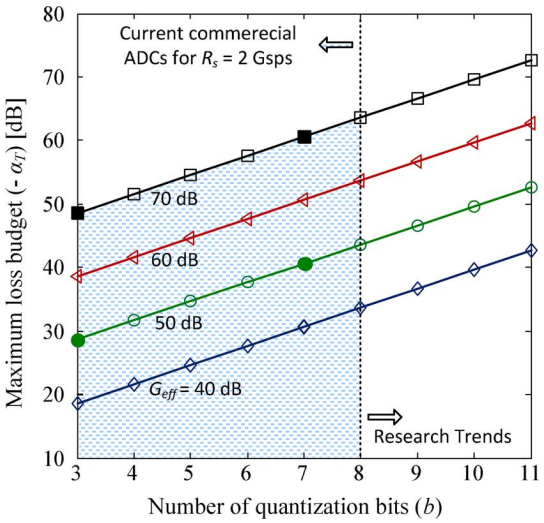

Fig. 7. Maximum loss budget as a function of the number of quantization bits and for different resistors.

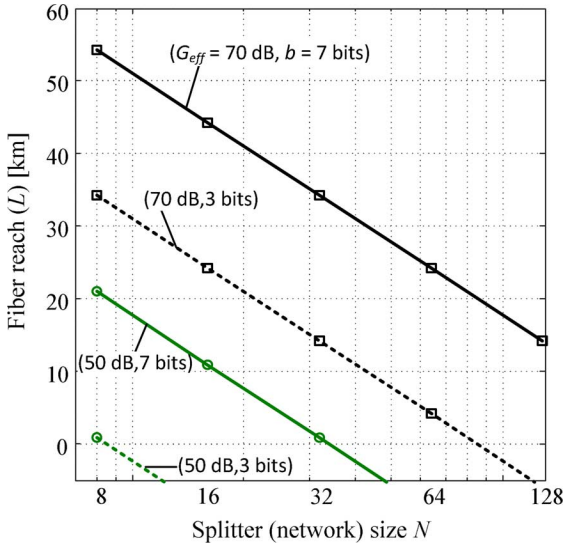

Fig. 8. Trade-off between the fiber reach and the splitter size at the RN for different values of the number of quantization bits and postamplification gain.

where the left side of (1) gives the voltage difference between the fourth and the fifth pulses of the periodic sequence at the ADC input. The total loss budget α_T that can be tolerated is

$$\alpha_T \geq 11\frac{V_{\text{ref}}}{RP_sG_{\text{eff}}2^b}. \tag{2}$$

Thus, the lower bound (maximum acceptable) of α_T is inversely proportional to $G_{\text{eff}}, 2^b$ and the detector responsivity R. It also depends on the peak of the launched power P_s.

Fig. 7 shows the minimum loss budget α_T versus the number of quantization bits b for different values of G_{eff}. For our numerical results, we consider $P_s = 10$ dBm, $R = 1$ and $V_{\text{ref}} = 1$ volts [12], [13]. The highlighted region corresponds to the current commercial TIAs and ADCs working at 2 Gs/s. Note that by employing high-gain avalanche photodetectors, the loss budget can be further improved [14], [15].

The total loss budget α_T is determined by the component losses as (in decibels)

$$-\alpha_T = 20\log_{10} N + 0.6L + \alpha_L \tag{3}$$

where N is the network size (total splitting size) and L is the fiber reach (sum of fiber feeder and longest drop fiber). A 0.3 dB/km of fiber loss is considered for U-band signals. The factor α_L is considered for the losses due to encoding, splicing, connectors, etc. An ideal periodic encoder imposes $\approx$5 dB loss [4]. A total value of 5 dB is assumed for other losses (mainly the connectors and splicings). Thus, the total loss is $\alpha_L = 10$ dB. Fig. 8 shows the trade-off between the fiber reach L in km and the splitter size at the RN for different G_{eff} and b (corresponding to the filled circles and squares in Fig. 7). The optical coding (OC) monitoring system is able to support the current PON standards [6], [7] such as a GPON with 64 customers and 20 km fiber reach.

V. Conclusion

We experimentally demonstrated fiber link quality monitoring of a PON using periodic codes for up to 16 customers. We demonstrated more robust monitoring for networks with a tiered geographic distribution by exploiting information about the distance separating clusters. Our experimental setup allows a capacity scale up for 64 customer PON. We also studied the final loss budget limitation of OC monitoring system as a function of the postdetection circuit specifications. We showed that the transimpedance gain and the number of ADC quantization bits play important roles in the total permissible loss budget. In addition, our numerical studies shows that OC monitoring technology is able to support the current PON standards.

References

[1] H. Fathallah and L. A. Rusch, "Code division multiplexing for in-service out-of-band monitoring," *J. Opt. Netw.*, vol. 6, no. 7, pp. 819–829, Jul. 2007.

[2] M. M. Rad, H. Fathallah, S. LaRochelle, and L. A. Rusch, "Experimental validation of PON monitoring using periodic coding," in *Proc. IEEE GLOBECOM*, Honolulu, HI, Feb. 2009, pp. 1–7, Paper ONS-04.6.

[3] N. Honda, D. Iida, H. Izumita, and Y. Azuma, "In-service line monitoring system in PONs using 1650 nm Brillouin OTDR and fibers with individually assigned BFSs," *IEEE J. Lightw. Technol.*, vol. 27, no. 20, pp. 4575–4582, Oct. 2009.

[4] H. Fathallah, M. M. Rad, and L. A. Rusch, "PON monitoring: Periodic encoders with low capital and operational cost," *IEEE Photon. Technol. Lett.*, vol. 20, no. 24, pp. 2039–2041, Dec. 2008.

[5] M. M. Rad, H. Fathallah, S. LaRochelle, and L. A. Rusch, "Computationally efficient monitoring of PON fiber link quality using periodic coding," *IEEE/OSA J. Opt. Commun. Netw.*, vol. 3, no. 1, pp. 77–86, Jan. 2011.

[6] A. Girard, "FTTx PON technology and testing," in *EXFO Electro-Opt. Eng. Inc.*, Canada, 2005.

[7] M. D. Vaughn, D. Kozichek, D. Meis, A. Boskovic, and R. Wanger, "Value of reach-and-split ratio increase in FTTH access networks," *IEEE J. Lightw. Technol.*, vol. 22, no. 11, pp. 2617–2622, Nov. 2004.

[8] D. Derickson, *Fiber Optic Test and Measurement*. Englewood Cliffs, NJ: Prentice-Hall, 1998.

[9] B. Razavi, *Design of Integrated Circuits for Optical Communication*. New York: McGraw-Hill, 2003.

[10] S. D. Personick, "Optical detectors and receivers," *IEEE J. Lightw. Technol.*, vol. 26, no. 9, pp. 1005–1020, May 2008.
[11] ONET8501, "Limiting transimpedance amplifier with RSSI," in Texas Instrument [Online]. Available: http://www.ti.com/
[12] S. Galal and B. Razavi, "10-Gb/s limiting amplifier and laser/modular driver in 0.18-μm CMOS technology," *IEEE J. Solid-State Circuits*, vol. 38, no. 12, pp. 2138–2146, Dec. 2003.
[13] R. H. Walden, "Analog-to-digital converter survey and analysis," *IEEE J. Sel. Areas Commun. (JSAC)*, vol. 17, no. 4, pp. 539–550, Apr. 1999.
[14] J. C. Campbell, "Recent advances in telecommunications avalanche photodiodes," *IEEE J. Lightw. Technol.*, vol. 25, no. 1, pp. 109–121, Jan. 2007.
[15] N. Gagnon, A. Girard, and M. Leblanc, "Considerations and recommendations for in-service out-of-band testing on live FTTH networks," in *Proc. IEEE Opt. Fiber Commun. Conf. (OFC)*, Mar. 2006, pp. 8–, Paper NWA3.
[16] M. Ismail, *Low Power Low Voltage Sigma Delta Modulators in Nanometer CMOS*. New York: Springer-Verlag, 2006.

Mohammad M. Rad (S'08–M'10) received the B.S.E.E. and M.S.C. degrees from the Sharif University of Technology, Tehran, Iran, in 2003 and 2005, respectively, and the Ph.D. degree from the Center for Optics, Photonics and Lasers (COPL), Université Laval, Quebec, QC, Canada, in 2010.

He is currently a Researcher at the University of Waterloo, Waterloo, ON, Canada. His research interests include fiber-optic telecommunications, network monitoring, passive optical networks, coherent optical communications, free-space optics, and sensor networks.

Julien Penon (M'09) received the *Diplme dtudes Approfondies* in optics and photonics from Université Paris XI, Orsay, France, in 2003. In 2009, he received the Ph.D. degree in optical telecommunications with a dissertation on spectral amplitude coded optical codedivision multiple-access (SAC-OCDMA) from the Center for Optics, Photonics, and Lasers (COPL), Department of Electrical and Computer Engineering, Université Laval, Quebec, Canada.

During his doctoral studies, he completed an internship directed by Mario J. Paniccia at Intels Silicon Photonics Research Lab concerning in silicon modulator design and testing. He is currently with Averna, Montreal, QC, Canada, a test and measurement company, where he is both an Optical Developer and Resource Person for optical telecommunications issues. In this position, he was involved in 40 G transponder testing with a major manufacturer.

Habib A. Fathallah (S'96–M'01) received the B.S.E.E.(Hons.) degree from the National Engineering School of Tunis, Tunis, Tunisia, in 1994, and the M.S.C. and Ph.D. degrees in electrical engineering from Université Laval, Quebec, Canada, in 1997 and 2001, respectively.

He initiated the use of Bragg gratings technology for all-optical/all-fiber coding/decoding in Optical CDMA systems. He was the founder of Access Photonic Networks (2001–2006). He is currently with the Department of Electrical Engineering, College of Engineering, King Saud University, Riyadh, Saudi Arabia, and an Adjunct Professor with the Department of Electrical and Computer Engineering, Laval University, Quebec, Canada. His research interests include optical communications systems and technologies, metro and access networks, Optical CDMA, passive optical networks (PONs) and long reach PONs, FTTH, network monitoring, and hybrid fiber wireless (FiWi) systems.

Sophie LaRochelle (M'00) received the B.Eng. degree in engineering physics from Université Laval, Sainte-Foy, QC, Canada, in 1987, and the Ph.D. degree in optics from the University of Arizona, Tucson, in 1992.

From 1992 to 1996, she was a Research Scientist at the Defense Research and Development Canada-Valcartier, where she was involved in the field of electro-optical systems. She is currently a Professor in the Department of Electrical and Computer Engineering, Université Laval, where she holds a Canada Research Chair in Optical Fiber Communications and Components. She is a member of the Center for Optics, Photonics and Lasers (COPL). Her current research activities are focused on active and passive fiber optics components for optical communication systems, including fiber Bragg gratings, optical amplifiers, and multiwavelength and pulsed fiber lasers. Her other research interests include packet-switched networks with photonic code processing, transmission of radio-over-fiber signals, and optical code-division multiple access.

Dr. LaRochelle is a member of the Optical Society of America and the IEEE Lasers and Electro-Optics Society.

Leslie A. Rusch (S'91–M'94–SM'00–F'10) received the B.S.E.E.(Hons.) degree from the California Institute of Technology, Pasadena, in 1980, and the M.A. and Ph.D. degrees in electrical engineering from Princeton University, Princeton, NJ, in 1992 and 1994, respectively.

In 1994, she joined the Department of Electrical and Computer Engineering, Université Laval, Québec, QC, Canada, where she is currently a Full Professor performing research in wireless and optical communications. She spent two years as the Manager of a group researching new wireless technologies at Intel Corp. from 2001 to 2002. Her research interests include optical-code-division multiple access and spectrum sliced wavelength division multiplexing using incoherent sources for passive optical networks; semiconductor and erbium-doped optical amplifiers and their dynamics; radio over fiber; and in wireless communications, high performance, reduced complexity receivers for ultrawideband systems employing optical processing.